MASARYKOVA UNIVERZITA
PŘÍRODOVĚDECKÁ FAKULTA
ÚSTAV CHEMIE

Bakalářská práce

BRNO 2017 **VOJTĚCH KOPECKÝ**

MASARYKOVA UNIVERZITA
PŘÍRODOVĚDECKÁ FAKULTA
ÚSTAV CHEMIE

Ab initio calculations of structural properties and stability of $TiSi_2$

Bakalářská práce

Vojtěch Kopecký

Vedoucí práce: doc. Mgr. Jana Pavlů, Ph.D. **Brno 2017**

Bibliografický záznam

Autor:	Vojtěch Kopecký Přírodovědecká fakulta, Masarykova univerzita Ústav chemie
Název práce:	Ab initio výpočty strukturních vlastností a stability TiSi2
Studijní program:	Chemie
Studijní obor:	Chemie
Vedoucí práce:	doc. Mgr. Jana Pavlů, Ph.D.
Akademický rok:	2016/2017
Počet stran:	vii+30
Klíčová slova:	Křemík; Titan; Disilicid titanu; Ab initio; fáze C54; fáze C49; fáze C40; Zobecněná gradientová aproximace; Teorie funkcionálu hustoty; VASP

Bibliographic Entry

Author:	Vojtěch Kopecký Faculty of Science, Masaryk University Department of chemistry
Title of Thesis:	Ab initio calculations of structural properties and stability of $TiSi_2$
Degree Programme:	Chemistry
Field of Study:	Chemistry
Supervisor:	doc. Mgr. Jana Pavlů, Ph.D.
Academic Year:	2016/2017
Number of Pages:	vii+30
Keywords:	Silicon; Titanium; Titanium disilicide; phase C54; phase C49; phase C40; Ab initio; Generalized gradient approximation; Density functional theory; VASP

Abstrakt

Tato bakalářská práci se věnuje ab initio výpočtům vlastností disilicidu titanu ve fázích C45, C49 a C40. Strukturní relaxací byly získány rovnovážné parametry jednotlivých fází a z energií odpovídajícím těmto parametrům byla zjištěna tvorná tepla jednotlivých fází vůči fázi C49 a vůči čistým prvkům ve standardním stavu.

Abstract

This thesis focuses on ab initio calculations of properties of titanium disilicide in the C54, C49 and C54 phases. Equilibrium structural parameters were obtained by structural relaxation and the heat of formation was evaluated with respect to the C49 phase and pure elements in their ground state.

MASARYKOVA UNIVERZITA
Přírodovědecká fakulta

ZADÁNÍ BAKALÁŘSKÉ PRÁCE

Akademický rok: 2016/2017

Ústav: Ústav chemie

Student: Vojtěch Kopecký

Program: Chemie

Obor: Chemie

Ředitel *Ústavu chemie* PřF MU Vám ve smyslu Studijního a zkušebního řádu MU určuje bakalářskou práci s názvem:

Název práce: Ab initio výpočty strukturních vlastností a stability TiSi2

Název práce anglicky: Ab initio calculations of structural properties and stability of TiSi2

Oficiální zadání:
Cílem práce je seznámit se s možnostmi kvantově-mechanických výpočtů vlastností pevných látek, které jsou následně využitelné k posouzení termodynamického chování studovaných materiálů. Práce je zaměřena na výpočty tvorných tepel vybraných fází a jejich rovnovážného uspořádání. Za použití pseudopotenciálového kódu VASP (Vienna Ab initio Simulation Package) bude studována stabilita struktur C49, C40 a C54.

Literatura:
JENSEN, Frank. *Introduction to computational chemistry*. 2nd ed. Chichester: John Wiley & Sons, 2007. xx, 599. ISBN 9780470011874.

GIUSTINO, Feliciano. *Materials modelling using density functional theory :properties and predictions*. Oxford: Oxford University Press, 2014. xiv, 286. ISBN 9780199662432.

Jazyk závěrečné práce: angličtina

Vedoucí práce: doc. Mgr. Jana Pavlů, Ph.D.

Datum zadání práce: 28. 2. 2017

V Brně dne: 28. 2. 2017

Souhlasím se zadáním (podpis, datum):

Kopecký
.....
Vojtěch Kopecký
student

Pavlů
.....
doc. Mgr. Jana Pavlů, Ph.D.
vedoucí práce

.....
doc. Mgr. Marek Nečas, Ph.D
zástupce ředitele Ústavu chemie pro pedagogické záležitosti

Poděkování

Tímto bych chtěl poděkovat doc. Mgr. Janě Pavlů, Ph.D. za její zájem, čas a hlavně trpělivost, kterou mi věnovala. Dále bych chtěl svému otci za jeho odborné rady a také Metacentru, za poskytnuté výpočetní zdroje.

Prohlášení

Prohlašuji, že jsem svoji bakalářskou práci vypracoval samostatně s využitím informačních zdrojů, které jsou v práci citovány.

Brno 26. května 2017 .....

Vojtěch Kopecký

Contents

Introduction

Titanium disilicide is a material extensively used in integrated circuit technology used in source/drain junctions, gates, local interconnects, Schottky diodes [1], Infrared image sensors [2] and other electronic devices as well as in jet engines [3]. During processing of $TiSi_2$ thin films, complications arises due to thermodynamical properties of titanium disilicide. The material first crystallizes in the undesirable C49 phase which has to be treated with high temperature in order to transform to the desired C54 phase [4]. However the C49 to C54 phase transformation becomes problematic with decreasing dimensions of the device. The problem of efficacy of the C49 to C54 phase transformation had drawn a great deal of attention. One of proposed solutions [5] utilizes a relatively uninvestigated C40 phase to bypass the C49 phase, allowing for direct and efficient formation of the phase C54.

The purpose of this thesis is to find equilibrium structural parameters of titanium disilicides in the C54, C49 and C40 phases and their heats of formation relative to the standard states of pure elements or with respect to the C49 phase using ab initio calculations. Density of states and bulk moduli of the three phases are also investigated.

Chapter 1

Ab initio methods

In theoretical chemistry, the term "ab initio" is describing group of methods relying on first principles of quantum mechanics without using empirical input. The term "ab initio" itself comes from Latin, meaning "From beginning" and was first used in 1950s by Craig and Parr in semi-empirical study of configuration interaction in benzene [6]. In 1970s development of theoretical chemist's main tool, the computer, and release of efficient ab initio programs like Gaussian or ATMOL had significantly improved potential of ab initio calculations and formed a new field of chemistry: computational chemistry.

1.1 Born-Oppenheimer approximation

Solving Schrödinger's equation in multi-electronic systems requires vast amounts of computational power. In order to keep complexity of calculations within technologically feasible margins, multiple approximations have to be introduced. One of the most important approximations in molecular quantum mechanics and solid state physics is the Born Oppenheimer approximation, also known as "clamped nuclei" approximation. Atomic nuclei are much heavier than the electrons, therefore wave functions of electrons and atomic nuclei can be separated [7, 8]

$$\Psi = \psi_{electrons} \times \psi_{nuclei}. \tag{1.1}$$

Within this approximation, the Hamiltonian of the system consists of two terms

$$\hat{H} = \hat{H}_{electrons} + \hat{H}_{nuclei}. \tag{1.2}$$

$\hat{H}_{nuclei}$ is contribution from the nuclear repulsions and is obtained from Coulomb's law

$$\hat{H}_{nuclei} = \sum_{A=1}^{M} \sum_{B>A}^{M} \frac{Z_A Z_B}{r_{AB}}, \tag{1.3}$$

where Z is proton number of individual nuclei and r is the distance between them; A and B run over the M nuclei.

The electronic Hamiltonian is

$$\hat{H}_{electrons} = \hat{T} + \hat{V}_{ne} + \hat{V}_{ee}, \tag{1.4}$$

where $\hat{T}$ stands for the operator of kinetic energy, $\hat{V}_{ne}$ stands for the operator of potential energy of electrons in Coulomb field of the nuclei and $\hat{V}_{ee}$ denotes the operator of energy of Coulomb repulsion between electrons. Writing explicitly all these terms we get

$$\hat{H}_{electrons} = -\frac{1}{2}\sum_{i=1}^{N}\nabla_i^2 - \sum_{i=1}^{N}\sum_{A=1}^{M}\frac{Z_A}{r_{iA}} + \sum_{i=1}^{N}\sum_{j>i}^{M}\frac{1}{r_{ij}}, \tag{1.5}$$

here A and B run over the M nuclei while i and j denote the N electrons in the system.

1.2 Hartree-Fock approximation

Hartree-Fock method [7,9,10] is commonly used to solve many-body problem in quantum mechanics. The core of the method in the case of many-electron system is an approximation of the ground state wave function Ψ_0 for N electrons by antisymmetric product of N orthonormal single-electron wave function ψ_i. The antisymmetry of the approximate wave function Ψ_{HF} is guaranteed by the form of the Slater determinant

$$\Psi_0 \approx \Psi_{HF} = \frac{1}{\sqrt{N!}}\begin{pmatrix} \psi_1(\mathbf{r_1}) & \psi_2(\mathbf{r_1}) & \cdots & \psi_N(\mathbf{r_1}) \\ \psi_1(\mathbf{r_2}) & \psi_2(\mathbf{r_2}) & \cdots & \psi_N(\mathbf{r_2}) \\ \vdots & \vdots & \ddots & \vdots \\ \psi_1(\mathbf{r_N}) & \psi_2(\mathbf{r_N}) & \cdots & \psi_N(\mathbf{r_N}) \end{pmatrix}. \tag{1.6}$$

The ground state wave function Ψ_{HF} is the minimum point of the Hartree-Fock energy functional

$$E[\Psi] \equiv \langle \Psi | \hat{H} | \Psi \rangle \tag{1.7}$$

in the space of the Slater wave functions. Consequently, the minimum value $E[\Psi_{HF}]$ of the energy functional (1.7) is the ground state energy within the Hartee-Fock approximation.

The functional $E[\Psi]$ can be written as

$$E[\Psi] = \sum_{i=1}^{N} H_i + \frac{1}{2}\sum_{i,j=1}^{N}(J_{ij} - K_{ij}), \tag{1.8}$$

H_i is energy of independent electrons in the field of nuclei

$$H_i = \int \psi_i^*(\mathbf{r})\left[-\frac{1}{2}\nabla_i^2 - V_{ext}(\mathbf{r})\right]\psi_i(\mathbf{r})\,d\mathbf{r}, \tag{1.9}$$

J_{ij} are the Coulomb integrals giving the energy of electronic repulsion

$$J_{ij} = \iint \psi_i(\mathbf{r_1})\psi_i^*(\mathbf{r_1})\frac{1}{r_{12}}\psi_j(\mathbf{r_2})\psi_j^*(\mathbf{r_2})d\mathbf{r_1}d\mathbf{r_2} \tag{1.10}$$

and K_{ij} are the exchange integrals that give the effect of electronic exchange

$$K_{ij} = \iint \psi_i^*(\mathbf{r_1})\psi_j(\mathbf{r_1})\frac{1}{r_{12}}\psi_i(\mathbf{r_2})\psi_j^*(\mathbf{r_2})d\mathbf{r_1}d\mathbf{r_2}. \tag{1.11}$$

In equations 1.10 and 1.11, the variable r_{12} denotes $|\mathbf{r_2} - \mathbf{r_1}|$.

1.3 Density functional theory

Density Functional Theory (DFT) [7, 11–13] is one of the most prominent methods used in ab initio calculations, preferably used in analysis of very large systems and modeling of materials. DFT constitutes fundamentally different way of analyzing a system as it treats electron density as a basic variable instead of wave function as classical methods do. This novel approach can drastically reduce complexity of calculation because electron density is a function of merely three variables while wave function is a function of 3N variables. The method itself started with two theorems, published by Hohenberg and Kohn in a manuscript called *"'Inhomogeneous electron gas"* [14]', which argue that energy is a functional of electron density. The theorems are stated as follows:

The first theorem, Proof of existence: The external potential $V_{ext}(\mathbf{r})$ *is unique functional of electron density* $n(\mathbf{r})$*; since in turn* $V_{ext}(\mathbf{r})$ *fixes Hamiltonian we see that the full many-particle ground state is a unique functional of* $n(\mathbf{r})$

The second theorem, Variational principle: The energy functional

$$E[n] \equiv \left\langle \Psi[n] \left| \hat{H} \right| \Psi[n] \right\rangle \tag{1.12}$$

delivers the true ground state energy of the system, if the input density is the true ground state density

$$E_0 = min_{n \in N} E[n]. \tag{1.13}$$

Let's substitute Hamiltonian from equation 1.4 into 1.12

$$E[n] = \left\langle \Psi[n] \left| \hat{T} + \hat{V}_{ee} + \hat{V}_{ne} \right| \Psi[n] \right\rangle. \tag{1.14}$$

If V_n is defined as Coulomb field of the nuclei, equation 1.14 can be expanded into

$$E[n] = \left\langle \Psi[n] \left| \hat{T} + \hat{V}_{ee} \right| \Psi[n] \right\rangle + \left\langle \Psi[n] \left| \sum_i V_n(\mathbf{r_i}) \right| \Psi[n] \right\rangle \tag{1.15}$$

Here we can see that the last term is clearly dependent on the electron density, but the other two terms, kinetic energy and energy of electron repulsion, are dependent only implicitly as follows from the first Hohenberg-Kohn theorem. The Hohenberg-Kohn functional, F_{HK}, groups these two $(\hat{T} + \hat{V}_{ee})$ terms together

$$E[n] = F_{HK}[n] + \int n(\mathbf{r})\, V_n(\mathbf{r})\, d\mathbf{r}. \tag{1.16}$$

Hohenberg-Kohn functional is also known as universal functional since it is universal to all many-body systems. Assuming the ground state is not degenerate F_{HK} determines the wave function and hence all values of a system. The functional is however of no use in actual calculations since it's exact form is still unknown.

Kohn and Sham [15] proposed to create a fictitious system consisting of non-interacting particles, that results the same ground state density as system of interacting particles. Lack of interaction between particles allows density to be assembled from single particle orbitals

$$n(\mathbf{r}) = \sum_{i=1}^{N} \langle \psi_i | \hat{n}(\mathbf{r}) | \psi_i \rangle . \tag{1.17}$$

The approximation to independent electrons turns solution of Shrödingers equation into relatively easy procedure, but would come at cost of severe inaccuracy. The idea of Kohn and Sham was to cover the cost of this approximation by adding another term into the equation of total energy, the exchange correlation energy E_{XC}, that would contain all non-classical phenomena

$$E[n] = T_C + V_H + E_{XC} + V_{ne}, \tag{1.18}$$

where the sum of expectation values of kinetic energy $\hat{T}$ and energy of electron interaction $\hat{V}_{ee}$ in equation 1.15 has been replaced by the sum of the kinetic energy of non interacting electrons T_C, the Hartree energy V_H (the classical interaction between electrons) and the exchange correlation energy E_{XC}.

The second Hohenberg-Kohn theorem guarantees that the functional derivative $\frac{\delta E[n]}{\delta n}$ is equal to zero for the ground state density. Thus, the ground state density can be determined from Kohn Sham equations

$$\left(-\frac{1}{2}\nabla^2 + V_{ne}(\mathbf{r}) + \int \frac{n(\mathbf{r}')}{|\mathbf{r}-\mathbf{r}'|} + v_{XC} \right) \phi_i(\mathbf{r}) = \varepsilon_i \phi_i, \tag{1.19}$$

where v_{XC} is exchange correlation function defined by

$$v_{XC} = \frac{\delta E_{XC}[n]}{\delta n}. \tag{1.20}$$

From Born's rule [16] wave function of orbitals is interpreted as electron density

$$\int d\mathbf{r} \sum_{i=1}^{N} |\phi(\mathbf{r})|^2 = \int d\mathbf{r}\, m(\mathbf{r}) = N \tag{1.21}$$

ϕ_i in the eq. 1.19 are the Kohn Sham orbitals and ε_i are their eigenvalues. Kohn Sham equations are solved iteratively because the eqs. 1.19, 1.21 and density in eq.1.20 are dependent on each other. Procedure used to solve Kohn-Sham equations is illustrated in Figure 1.1

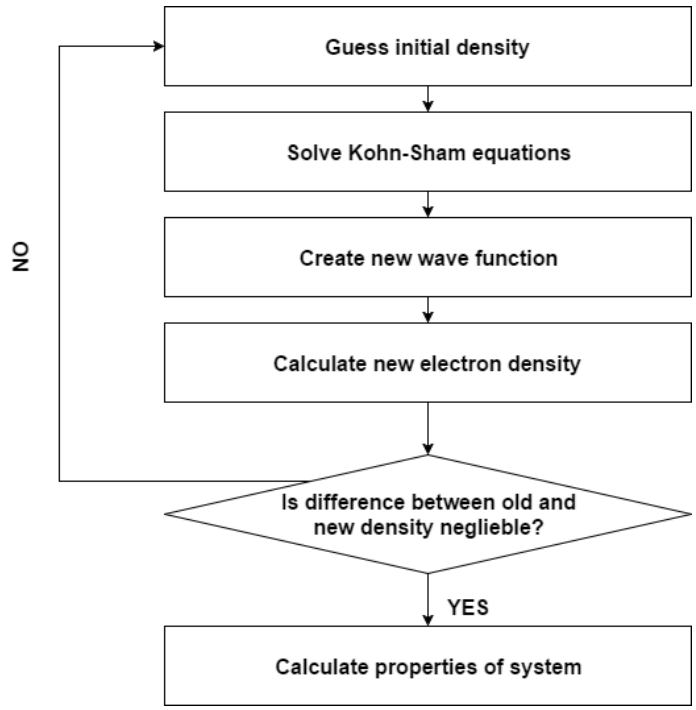

Figure 1.1: Kohn-Sham scheme

1.3.1 Local density approximation

Local density approximation, or shortly LDA, is the oldest method of approximating exchange-correlation energy. LDA is based on assumption that energy of exchange and correlation can be approximated as sum of exchange-correlation energies of infinitely small areas of constant densities, where the electrons would behave like homogenous electron gas. Total exchange and correlation energy of system is, therefore,

$$E_{XC}^{LDA}[n] = \int_V n(\mathbf{r})\varepsilon_{XC}(n(\mathbf{r}))dV, \tag{1.22}$$

where $\varepsilon_{XC}(n(\mathbf{r}))$ stands for exchange-correlation energy of infinitely small volume of homogenous electron gas.

Within the model of homogenous electron gas energy of exchange is known exactly

$$E_X = -\frac{3}{4}\left(\frac{3}{\pi}\right)^{\frac{1}{3}} \int_V n^{\frac{4}{3}}(\mathbf{r})\, d\mathbf{r}. \tag{1.23}$$

Estimating correlation energy is a more difficult matter as it can only be found analytically within the limits of extremely low or extremely high densities. Fortunately it was calculated numerically using quantum Monte-Carlo techniques [17, 18] .

From principle of the method it can be expected that LDA would only be reliable when applied to systems with slowly varying electron densities, but as it usually overestimates the correlation energy and underestimates exchange energy, it's errors often happen to negate each other, thus the method can lead to correct results by accident. One of most notable systematic error of LDA is underestimation of lattice parameters.

1.3.2 Generalized gradient approximation

Next step in approximating exchange correlation energy is Generalized Gradient Approximation, or shortly GGA. GGA extends LDA by accounting not only for electron density, but also for gradient terms of electron density. Exchange correlation energy can be formulated by following equation

$$E_{XC}^{GGA} = \int f(n, \nabla n)\, d(\mathbf{r}). \tag{1.24}$$

Contrary to LDA, common error of GGA is overestimation of lattice parameters.

1.4 Pseudopotential plane wave approach

Pseudopotential plane wave approach is an effective way of calculating properties of crystalline solids. Within pseudopotential plane wave approach [19, 20] single particle Kohn Sham wave functions in crystalline solids are expanded into a basis set of plane wave functions (Bloch functions), therefore Schrödinger's equation takes form of linear equations. Expansion coefficients are solution of the linear equations.

Problem arises from wave functions in core regions, that have complicated nodal structure, which would make practical calculations very difficult. Hence the pseudopotential approximation is introduced. Basis of this approximation is an observation, that the interactions between atoms in material are influenced by valence electrons to a much greater extend than by electrons in core. Pseudopotential approximation exploits it by "freezing" core electrons, eg. core electrons only act as static shielding to the electrostatic potential of the nuclei. The most general form of pseudopotential is

$$\hat{V}_{pseud} = \sum_{lm} |lm\rangle \hat{V}_l \langle lm|, \tag{1.25}$$

where $|lm\rangle$ are spherical harmonics and V_l is the pseudopotential for angular momentum l.

Illustrative example of pseudopotential wave function and corresponding Coulomb potential are depicted in Figure 1.2.

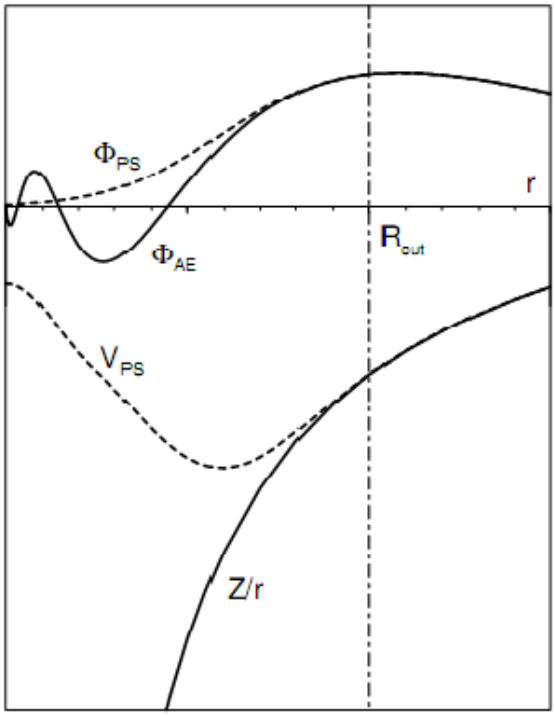

Figure 1.2: Illustration of an atomic wave function of all electrons (solid line) compared to atomic pseudo wave function (dashed line) and their respective Coulomb potential and pseudopotential [20]

1.5 VASP

Vienna ab initio simulation package, or shortly VASP [21, 22], is a program used for ab initio modeling of materials at atomic scale. Development of VASP started in 1991 and was based on early version of CASTEP code. VASP solves Schrödinger's equations either using density functional theory by solving Kohn-Sham equations, or with Hartree-Fock approximation. There are also implemented hybrid functionals that mix Hartree-Fock approach with density functional theory. Interactions between particles are calculated utilizing either ultra-soft or norm-conserving pseudopotentials; or projector augmented wave method.

Chapter 2

Properties of materials

2.1 Titanium

Titanium is a metal with silver color belonging to group 4 of periodic table with exceptional strength to density ratio. It was first discovered in 1791 by an English clergyman and amateur chemist William Gregor and is the 9th most abundant element in Earth's crust, occurring in the forms of oxides or silicates [23]. Titanium has two common allotropic modifications: α, hexagonal close packed structure stable in temperatures under 882°C and β, body centered cubic structure, stable within 882-1660 °C [24]. In this thesis the α modification is used as the ground state of titanium. On figures in this thesis titanium shall be marked by gray colour. Structure of α titanium is illustrated in Figure 2.1

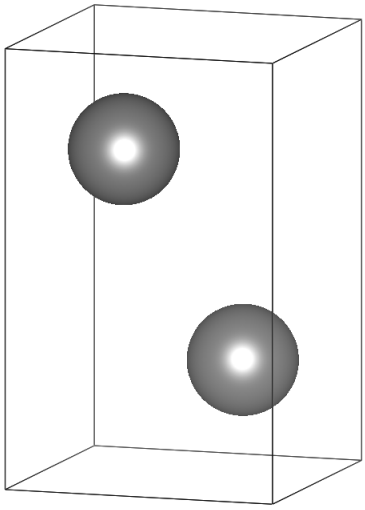

Figure 2.1: Structure of α titanium

2.2 Silicon

Silicon is a metalloid element from group 14 of periodic table. In it's pure form it is brittle, hard crystalline solid with gray-blue luster [25]. Silicon as an element was first identified by Swedish chemist Jöns Jakob Berzelius in 1823. Despite being the 2nd most common element in Earth's crust, silicon is almost never found in its elemental form, but in the form of various silicates, for which is responsible element's high affinity to oxygen [23]. Elemental silicon crystallizes in diamond cubic (DIA) structure. It has no other common allotropic modifications, but the tetrahedral angles deform under high pressure [23]. On figures in this thesis silicon shall be marked by blue color. Structure of silicon is illustrated in Figure 2.2.

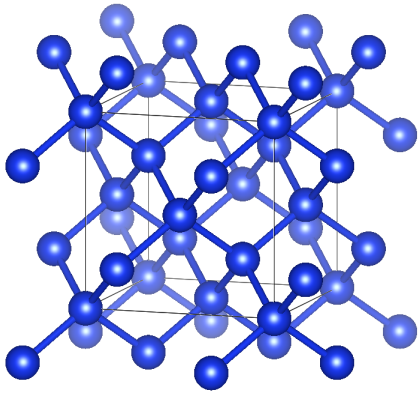

Figure 2.2: Structure of DIA silicon

2.3 Titanium disilicide

Titanium disilicide is an intermetallic compound used in electronic industry in a form of thin films as material for contact metallisation. It has exceptionally low electrical resistance, great contact with other materials in electronic circuits and it's ability to tolerate high temperatures and numerous chemical agents necessary in production. High solubility of oxygen in titanium is another favourable property, since it can reduce native oxides contaminating the substrate [26, 27]. Three phases of titanium disilicide are known: C54, C49 and C40; the phases are described in Tables 2.1 and 2.2.

Phase	Crystal structure	Space group	Lattice parameters			Resistivity
			a [Å]	b [Å]	c [Å]	$[\mu\Omega cm]$
C54	Orthorhombic face centered	Fddd	8.63	4.80	8.55	3-4
C49	Orthorhombic base centered	Cmcm	3.55	13.49	3.55	50-70
C40	Hexagonal	$P6_422$	4.70	4.70	6.49	22

Table 2.1: Overview of different structures [28–30] of $TiSi_2$ and their respective resistivity [31]; for practical reasons lattice parameters were rounded to 0.01 Å

Phase	Site	Multiplicity	Wyckoff	x	y	z
C54	Si	16	f	1/8	0.462	1/8
	Ti	8	a	1/8	1/8	1/8
C49	Si1	4	c	0	0.061	1/8
	Si2	4	c	0	0.750	1/8
	Ti	4	c	0	0.396	1/8
C40	Si	6	d	1/2	0	1/2
	Ti	3	j	1/6±Δ	1/3±2Δ	1/2

Table 2.2: Atom coordinates of different structures of $TiSi_2$ [28, 29]; the C40 structure tends to stray from ideal [32, 33], Δ shows what form of deviation is expected

2.3.1 C54

The C54 phase is a face centered orthorhombic structure and, according to the experiments, the stable structure of $TiSi_2$ [34]. The C54 phase has excellent electrical resistivity of 3-4 $\mu\Omega$ cm [31] compared to other transitional metal disilicides, which makes is it desirable in technological applications. Structure of C54 phase is shown in Figure 2.3.

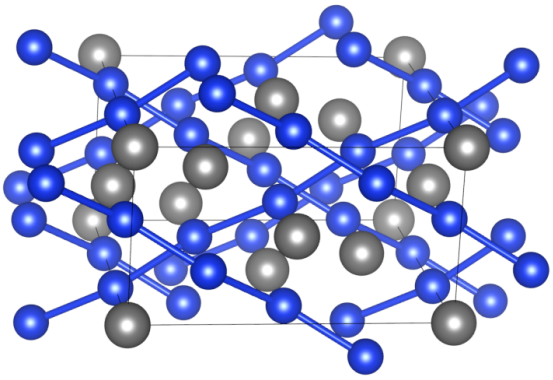

Figure 2.3: Structure C54

2.3.2 C49

The metastable C49 phase is a base centered orthorhombic structure, that often forms prior to the C54 phase, which hampers fabrication of devices using $TiSi_2$. Kinetic factors are deemed to be the cause of this. [34–36]. Ab initio calculations had shown formation energy of C49 phase to be the similar to C54 phase [37–39]. The C49 phase possesses the largest electrical resistivity out of the three phases: 50-70 $\mu\Omega$ cm [31] and was reported to be highly susceptible to defects [40,41]. Structure of C49 phase is shown in Figure 2.4.

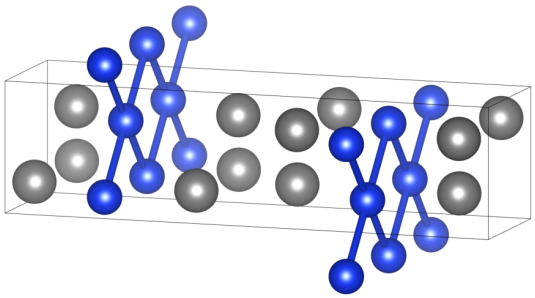

Figure 2.4: Structure C49

2.3.3 C40

The C40 phase is a relatively newly discovered hexagonal structure of $TiSi_2$, that shows potential as template structure [42] for formation of the technologically important C54 phase. Ab initio calculations [37] had shown it to be the least stable out of the three structures . The electrical resistivity of C40 is 22 $\mu\Omega$ cm [31]. Structure of the C40 phase is shown in Figure 2.5

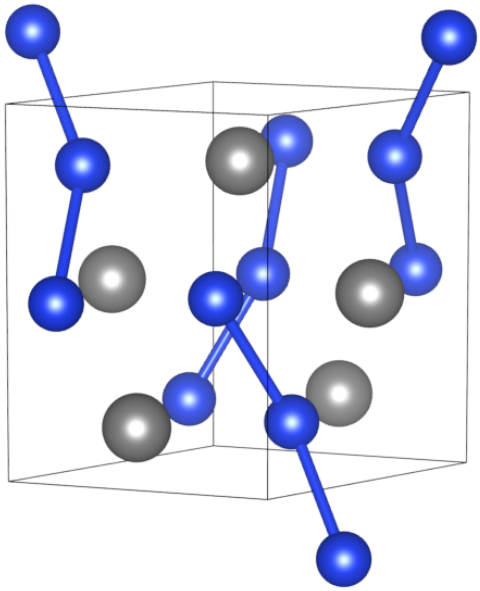

Figure 2.5: Structure of C40 phase

Chapter 3

Results and disscusion

Calculations in this thesis were done with VASP code version 5.3 employing Projector Augmented Wave - Perdew - Burke - Erzerhof pseudopotentials [43–45]. Out of PAW potentials for titanium only 3*d* and 4*s* orbitals were treated as valence shells and for silicon it was the 3*s* and 3*p* orbitals. Exchange-correlation energy was calculated within the frame of Generalized Gradient Approximation.

For better performance and accuracy of results, influence of technical parameters KSPACING and ENCUT on total energy was analyzed. Testing calculations were done on structures with experimental lattice parameters, therefore the energies of compressed structures is lower than the uncompressed ones.

3.1 Technical parameters

3.1.1 KSPACING parameter

An automatic generation of k-point mesh was chosen for calculations in this thesis. The optimal setting of KSPACING parameter, determining the density of k-points was chosen based on test calculations where the dependence of total energy on value of KSPACING parameter was studied. Once convergence was reached, the optimal value of KSPACING parameter was chosen. Here we used convergence criterion 10^{-5} eV per atom. Optimization process was done for all three phases and for each of them two unit cells (the first one in 100% and the second one in 95% of experimental volume) were used. Data obtained during optimization procedure are shown in Figures 3.1, 3.2 and 3.3.

The optimal value of KSPACING parameter was found to be 0.075, corresponding to 360, 676 and 336 irreducible k-points for structures C54, C49 and C40, respectively.

3.1.2 ENCUT parameter

ENCUT parameter sets the cut-off energy in eV for plane wave basis set. All plane waves with energy larger than the cut-off energy are ignored. ENCUT parameter was determined similar to KSPACING parameter with the same convergence criterion. Data obtained during optimization procedure are shown in Figures 3.4, 3.5 and 3.6. ENCUT 650 was found to be optimal, corresponding to cut-off energy of 650 eV.

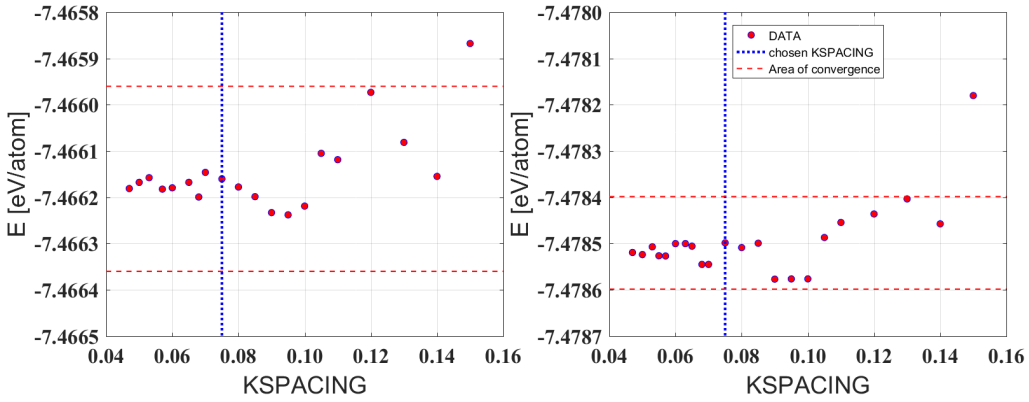

Figure 3.1: Dependence of total energy on KSPACING parameter for the C54 phase; On the left in 100% and on the right in 95% of volume

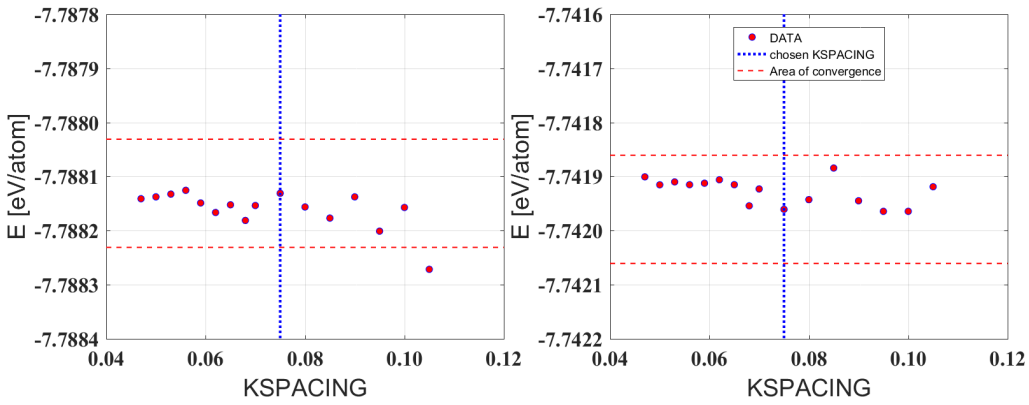

Figure 3.2: Dependence of total energy on KSPACING parameter for the C49 phase

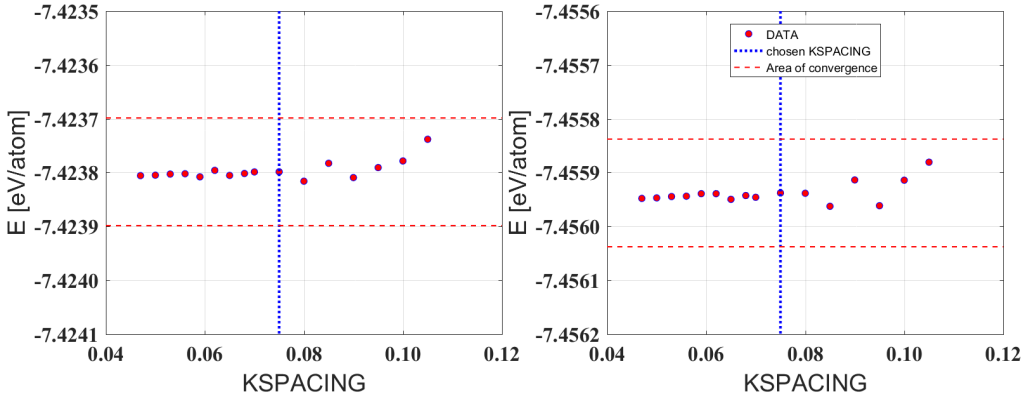

Figure 3.3: Dependence of total energy on KSPACING parameter for the C40 phase

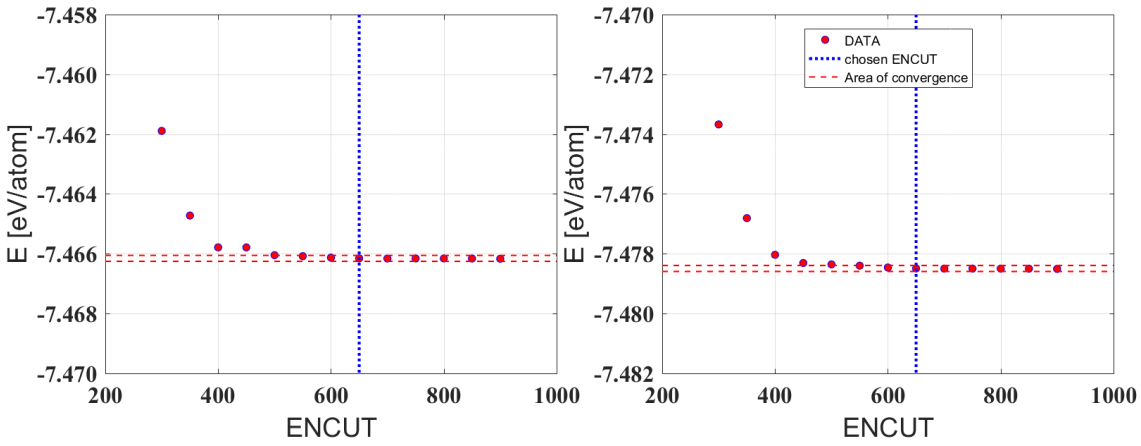

Figure 3.4: Dependence of total energy on ENCUT parameter for the C54 phase; On the left in 100% and on the right in 95% of volume

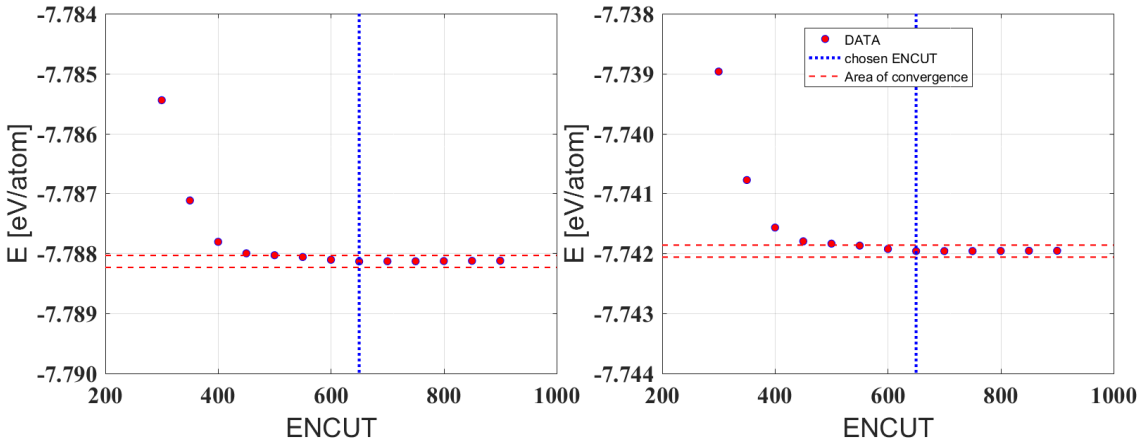

Figure 3.5: Dependence of total energy on ENCUT parameter for the C49 phase

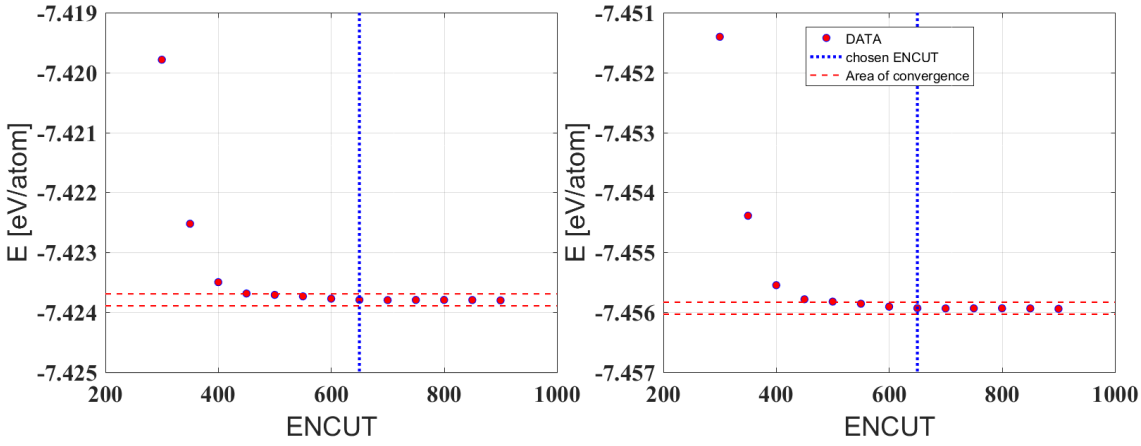

Figure 3.6: Dependence of total energy on ENCUT parameter for the C40 phase

3.2 Relaxation

For calculations of material's properties, the structural parameters obtained from experiment need to be optimized in relaxation procedure. During the procedure forces acting on atoms in cell are found and then atoms are moved. Once the forces are minimized, it is assumed that structure is in a local minimum of potential energy. Such equilibrium structures are found at temperature of 0 K, thus it is expected that they will be smaller than the experimental ones, due to thermal expansion. The data obtained by structural relaxation of elemental silicon and titanium are listed in Table 3.1, lattice parameters from structural relation of the three phases of $TiSi_2$ are listed in Table 3.2. The internal parameters of structures were also relaxed, results are place below in Table 3.3.

Element	n	Cell parameters a [Å]	c [Å]	V [Å^3 /atom]	V/V$_{calc}$[%]	Ref.
Ti (α)	2	2.854	4.520	15.95	100.0	This work
Ti (α)	2	2.942	4.676	17.64	110.6	[46] exp.
Ti (α)	2	2.951	4.684	17.67	110.8	[47] exp.
Ti (α)	2	2.86	4.519	16.01	100.5	[48] LDA
Ti (α)	2	2.94	4.645	17.39	109.0	[48] PBE
Si (DIA)	8	5.403	5.403	19.72	100.0	This work
Si (DIA)	8	5.431	5.431	20.03	101.6	[49] exp.
Si (DIA)	8	5.431	5.431	20.03	101.6	[50] exp.

Table 3.1: Structural parameters of Ti and Si; n marks number of atoms in a cell; V/V$_{calc}$ marks the ratio between volume and volume calculated in this work

Results of relaxation of α titanium (Table 3.1) greatly underestimate volume of α titanium by roughly 10 % compared to experimental data [46, 47]. U. Argaman et al. arrived to similarly unrealistic results by using LDA method [48]. Calculated lattice parameters of silicon however do agree with experimental data [49, 50] within tolerable difference of 1.6 % of volume.

Structure	n	Cell parameters a [Å]	b [Å]	c [Å]	V/atom [Å]	V/V_{calc}[%]	Ref.
C54	24	8.125	4.728	8.448	13.52	100.0	This work
C54	24	8.116	4.721	8.443	13.48	99.7	[37] LDA
C54	24	8.268	4.806	8.56	14.17	104.8	[37] GGA
C54	24	8.140	4.774	8.483	13.74	101.6	[39] GGA
C54	24	8.179	4.605	8.470	13.29	98.3	[51] GGA
C54	24	8.268	4.800	8.552	14.14	104.6	[52] exp.
C54	24	8.267	4.800	8.551	14.14	104.6	[28] exp.
C49	12	3.487	13.262	3.537	13.63	100.0	This work
C49	12	3.489	13.256	3.528	13.60	99.8	[37] LDA
C49	12	3.541	13.617	3.576	14.37	105.4	[37] GGA
C49	12	3.514	13.383	3.534	13.85	101.6	[39] GGA
C49	12	3.509	13.507	3.531	13.85	101.6	[51] GGA
C49	12	3.56	13.61	3.56	14.37	106.3	[4] exp.
C49	12	3.55	13.49	3.55	14.14	104.6	[29] exp.
C40	9	4.654	4.654	6.500	13.55	100.0	This work
C40	9	4.65	4.65	6.496	13.52	99.7	[37] LDA
C40	9	4.731	4.731	6.572	14.15	104.5	[37] GGA
C40	9	4.674	4.674	6.532	13.66	100.8	[51] GGA
C40	9	4.67	4.67	6.62	13.89	102.5	[53] exp.
C40	9	4.698	4.698	6.492	13.79	101.8	[30] exp.
C40	9	4.71	4.71	6.56	13.94	102.9	[54] exp.

Table 3.2: Lattice parameters parameters of $TiSi_2$; n marks number of atoms in cell, V/V_{calc} marks the ratio between volume and volume calculated in this work

Structure	Si (16e) y	1Si(4c) y	2Si (4c) y	Ti (4c) y	1Si (6j) x	Ref.
C54	0.4608	N/A	N/A	N/A	N/A	This work
C54	0.4615	N/A	N/A	N/A	N/A	[28] exp.
C54	0.462	N/A	N/A	N/A	N/A	[55] GGA
C54	0.463	N/A	N/A	N/A	N/A	[37] GGA
C54	0.462	N/A	N/A	N/A	N/A	[37] LDA
C49	N/A	0.0597	0.7495	0.3976	N/A	This work
C49	N/A	0.103	0.750	0.441	N/A	[55] GGA
C49	N/A	0.1022	0.7523	0.4461	N/A	[39] GGA
C49	N/A	0.061	0.750	0.396	N/A	[29] exp.
C40	N/A	N/A	N/A	N/A	0.1629	This work
C40	N/A	N/A	N/A	N/A	0.1658	[56]*Ta
C40	N/A	N/A	N/A	N/A	0.1593	[33]*Nb
C40	N/A	N/A	N/A	N/A	0.1658	[33]*Cr

Table 3.3: Internal parameters of $TiSi_2$ in different phases; *M marks that the data are from structure of different disilicide MSi_2, N/A indicates that the internal parameter is not present in structure

Calculated lattice parameters of the C54 and C49 phases stand apart from experimental data with significant discrepancy of 4.6-6.3 % of volume. Ab initio calculations done on CASTEP code yielded [39,51] similar result varying only by 1.6% of volume. Best match with experimental data had Colinet et al. using VASP code with GGA [37]. In contrast internal parameters of C54 structure agreed well with both experimental data [28] and ab initio calculation [37, 55]. Surprisingly internal parameters of calculated C49 phase correspond to experimental data [29] better than other Ab initio calculations [39, 55].

Underestimation of lattice parameters in structure of C40 phase compared to experimental data [30, 53, 54] appears to be within tolerable margins of 1.8-2.9 % of volume. Lattice parameters from ab initio calculations performed by CASTEP again do agree with lattice parameters obtained in this thesis [51], C. Colinet et al. [37] on VASP code with GGA on the other hand overestimate lattice parameters, although by smaller amount. Unfortunately no data on internal parameters of $TiSi_2$ in C40 phase could be found thus they can be only compared to internal parameters of other disilicides in the same structure. From experiments it is known that the (6j) x parameter in silicon sublatice for disilicides in the C40 structure oscillates around $\frac{1}{6}$ [33, 56]. Calculated internal parameter therefore fits well.

Overestimation of lattice parameters in phases C49, C54 and α titanium might be due to approximation semi-core orbital $3p$ by pseudopotentials. Colinet et al. [37] did treated semi-core orbital $3p$ as a valence orbital and achieved much better agreement with the experimental data.

3.3 Enthalpy of formation

The enthalpy of formation was calculated as a difference between weighted ratio of total energies of ground states of pure elements and energy of relaxed binary phases. Obtained data are listed in Tables 3.4 and 3.5.

Structure	Enthalpy of formation (H) [eV/f.u.]	[kJ/mole of f.u.]	Ref.
C49	-2.018	-194.7	This work
C49	-1.734	-167.3	[38] ABINIT GGA
C49	-1.595	-153.9	[55] VASP GGA
C49	-1.772	-171.0	[57] CALPHAD
C49	-1.664	-160.5	[39] CASTEP GGA
C49	-1.772	-171,0	[51] CASTEP GGA
C49	-1.506	-145.3	[51] DMol GGA
C54	-1.986	-191.6	This work
C54	-1.662 ± 0.051	-160.5 ± 5	[58] exp.
C54	-1.551	-149.6	[55] VASP GGA
C54	-1.709	-167.3	[38] ABINIT GGA
C54	-1.814	-175.1	[57] CALPHAD
C54	-1.666	-160.6	[39] CASTEP
C54	-1.700	-164.0	[51] CASTEP
C54	-1.445	-145.3	[51] DMol GGA
C40	-1.935	-186.7	This work
C40	-1.504	-145.1	[55] VASP GGA
C40	-1.661	-160.3	[51] CASTEP
C40	-1.405	-135.5	[51] DMol GGA

Table 3.4: Enthalpy of formation of different phases of $TiSi_2$ relative to pure elements

Structure	Enthalpy of formation (H) [eV/f.u.]	[kJ/mole of f.u.]	Ref.
C54	0.032	3.1	This work
C54	0.030	2.9	[37] VASP LDA
C54	0.047	4.5	[37] VASP GGA
C54	0.038	3.7	[37] FLAPW GGA
C54	-0.0009	-0.0087	[39] CASTEP
C54	0.072	7.0	[51] CASTEP
C54	0.061	5.9	[51] DMol GGA
C54	-0.45	-43	[34] MD
C54	-0.041	-4.1	[57] CALPHAD
C40	0.083	8.0	This work
C40	0.082	7.9	[37] VASP LDA
C40	0.090	8.7	[37] VASP GGA
C40	0.068	6.6	[37] FLAPW GGA
C40	0.111	10.7	[51] CASTEP
C40	0.101	9.8	[51] DMol GGA

Table 3.5: Enthalpy of formation of different phases of $TiSi_2$ relative to C49 phase

Results indicate that the C49 phase is the ground state of $TiSi_2$ at temperature of 0 K, followed by the C54 phase and the C40 phase is the least stable, which is consistent with most ab initio calculations [37,51,55], but in contradiction with ab initio calculations performed on CASTEP code by T. Wang et al. [39] and studies using the semi-empirical methods MD [34] and CALPHAD [57]. According to C. Colinet et al. [55], disagreement with these previous studies [34, 57] might be due to these studies using biased empirical input in order to get better agreement with experiments that treat the C54 phase as the ground state [36].

Obtained values of enthalpy of formation with respect to the pure elements in their standard state, diverge from both experimental data [58] and theoretical data from ab initio calculations [38,39,51,55,57] in greater extent. The deviation from studies [37], that used the same method as calculations in this thesis (VASP GGA), is 30 % on average, which is quite high value. Nonetheless even the data in literature are quite variable.

When C49 is taken as reference the enthalpies of formation do conform with other studies [37, 51, 57]. It should be mentioned that the FLAPW and DMol are full-potential methods, and therefore should be taken as the most accurate result of their respective studies.

From disparity between accuracy of enthalpies when different references are used, it can be concluded that the calculation of elements in their ground state was flawed. Large overestimation of the lattice parameters of α titanium would support this.

3.4 Density of states

In the band theory of crystalline solids, the Density of States (DOS) is defined as the number of available energy states per unit energy per unit volume [59, 60]. The density of states $n(E)$ for an energy E can be calculated based on knowledge of the electronic band structure of the solid using following equation

$$n(E) = \frac{1}{\Omega_{BZ}} \sum_{\nu} \int_{BZ} d\mathbf{k}\, \delta(E - E_{\nu}(\mathbf{k})). \tag{3.1}$$

In equation 3.1, the integral is taken over Brillouin zone with volume Ω_{BZ} and $E_{\nu}(\mathbf{k})$ is the electron energy for wave vector $\mathbf{k}$ in the band ν. Calculated density of states of the C54, C49 and C40 phase of $TiSi_2$ are illustrated in Figures 3.7, 3.8 and 3.9.

Our results compare well with data from other studies [51, 61, 62]. Only serious disparity was the band gap at 2 eV in the DOS of the C40 phase as the DOS from study by G. Shao [51] does not show any band gaps.

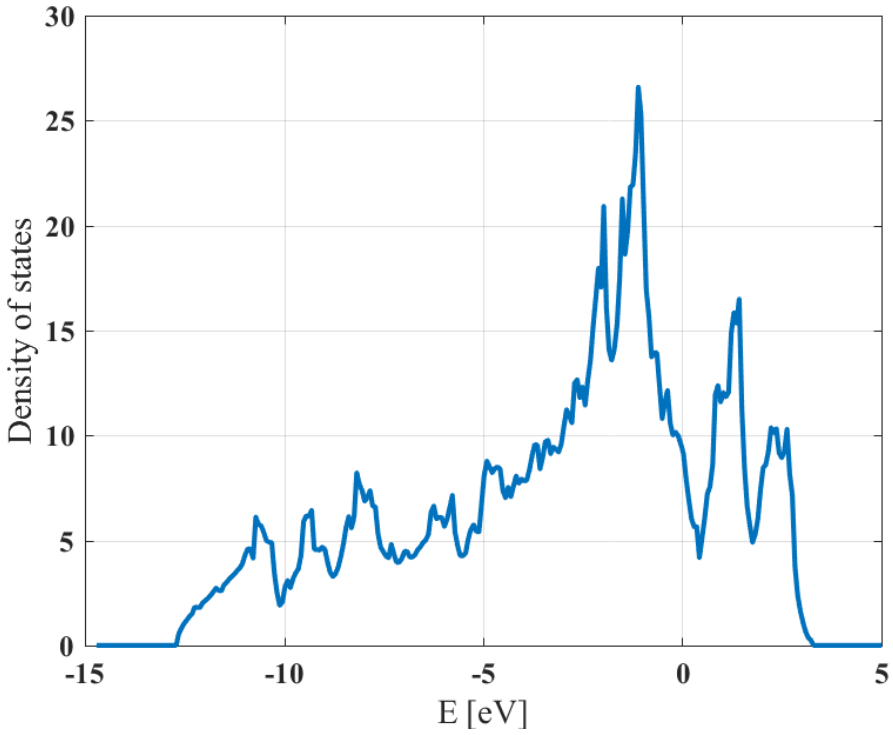

Figure 3.7: Density of states for C54 phase; Energy is zeroed to the Fermi level

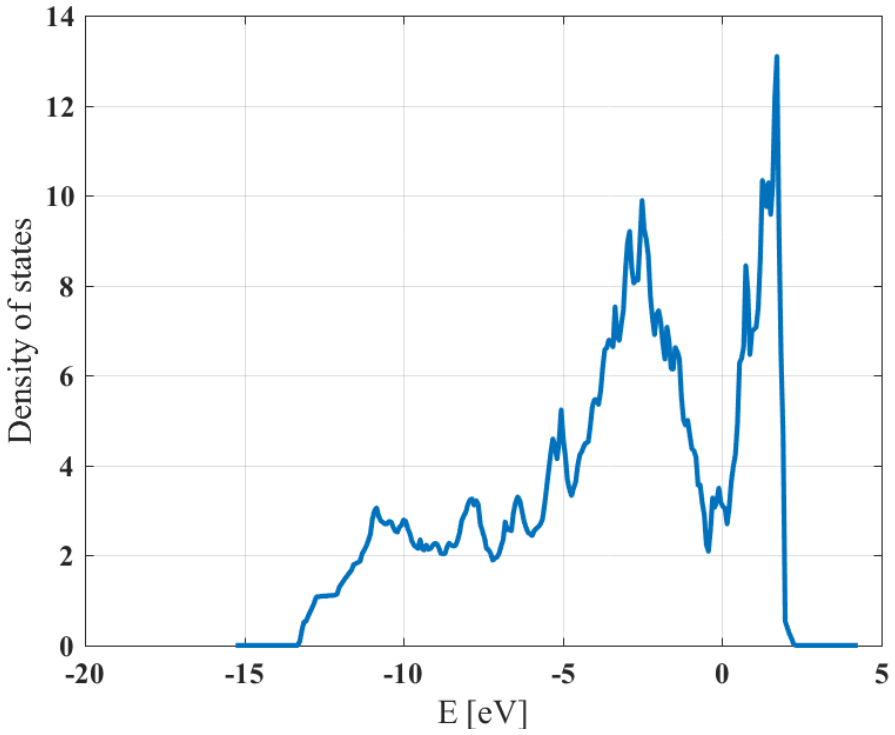

Figure 3.8: Density of states for C49; Energy is zeroed to the Fermi level

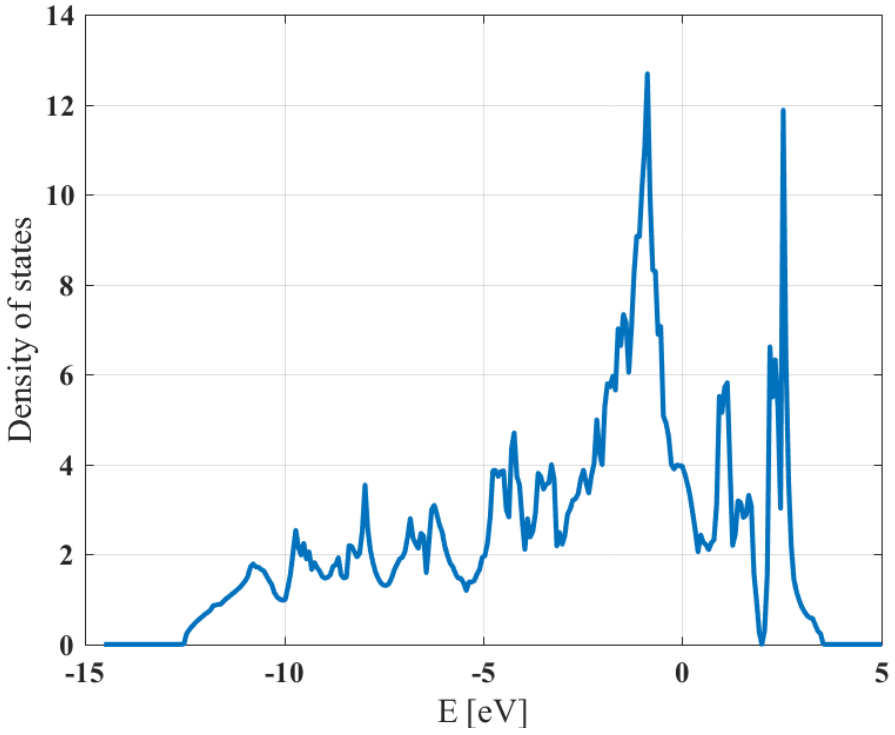

Figure 3.9: Density of states for C40 phase; Energy is zeroed to the Fermi level

3.5 Bulk moduli

Bulk modulus measures resistance of a substance to uniform compression. In this thesis bulk moduli are calculated by fitting multiple points by the Murnaghan equation of states to the calculated set of points showing the dependence of total energy on unit cell volume. The Murnaghan Equation of States, EOS, is defined as follow:

$$E = E_T + \frac{B_0 V}{B_0'}\left[\frac{(V_0/V)^{B_0'}}{B_0' - 1} + 1\right] - \frac{V_0 B_0}{B_0' - 1}, \tag{3.2}$$

where B_0 and B_0' are the bulk modulus and its pressure derivative at the equilibrium volume V_0.

Graphical results of the fit are shown in Figure 3.10 and bulk moduli from the fit are listed in Table 3.6.

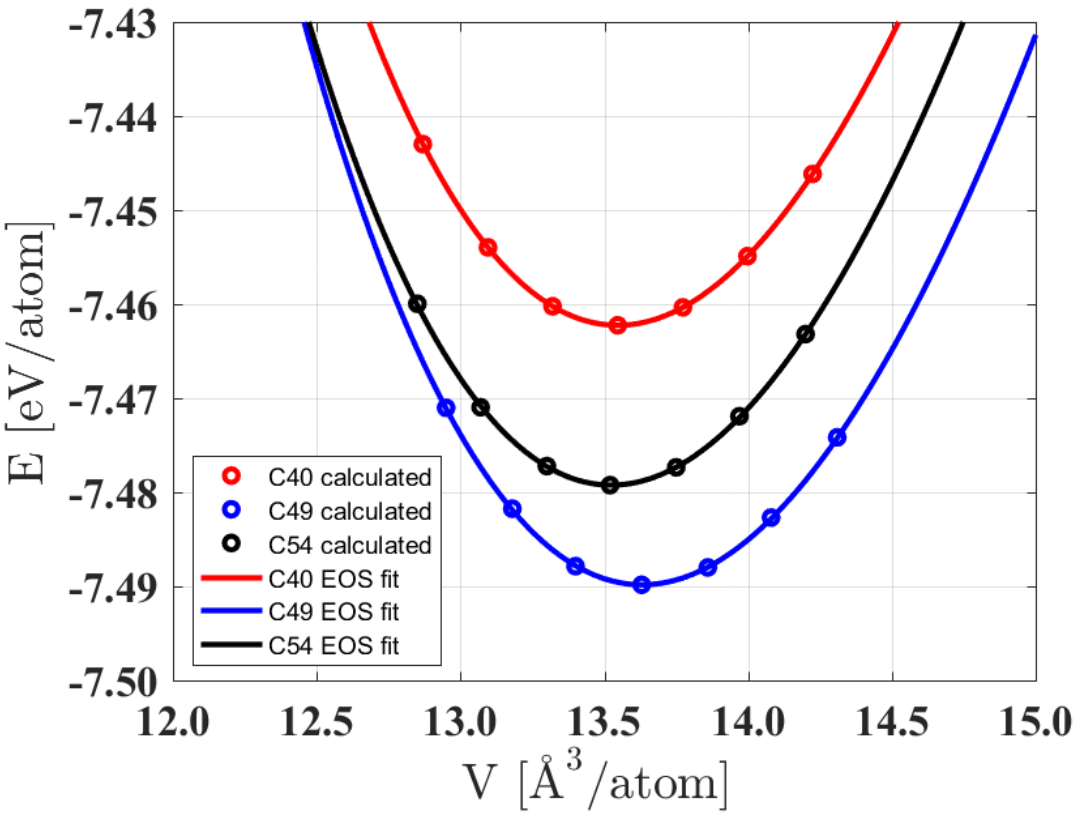

Figure 3.10: Dependence of total energy on volume

Bulk modulus calculated in this work for C54 phase was larger but comparable to experimental data [65–67]. But since experimental data for bulk modulus of the C54 phase range from 126.9 GPa [66] to 155± 2 GPa [67], the difference seems negligible. Moreover if experimental data are judged solely by age and result of C. Li et al. [67] would be taken as the most accurate, then the calculated bulk modulus of the C54 phase would show better agreement than other theoretical studies [63, 64].

B_{C54} [GPa]	B_{C49} [GPa]	B_{C40} [GPa]	Ref.
166.2	161.0	164.9	This work
126	94.6	N/A	[63] CASTEP GGA
176.4	153.9	N/A	[64] LMTO
146.8	102.9	N/A	[65] exp.
126.9	N/A	N/A	[66] exp.
155 ± 2	N/A	N/A	[67] exp.

Table 3.6: Bulk moduli

Calculated bulk modulus for the C49 phase was much larger than the one obtained from experiment [65]. A linear muffin-tin orbital study by M. Ekman and O. Vidvuds [64] does largely overestimates the bulk modulus too and the CASTEP GGA study by T. Wang et al. [63] does underestimate it by a little, but overall shows the best agreement with the experimental data.

Unfortunately no reference data were found for bulk modulus of the C40 phase.

Conclusion

In this thesis equilibrium structural parameters of the C54, C49 and C40 phases of $TiSi_2$ were obtained. Difference between the calculated lattice parameters and experimental data was significant. Compared to experimental data, our results overestimate volume of the C54 phase by 4.6 % [28, 52], the C49 phase by 4.6-6.3 % [4, 29] and the C40 phase by 2.5-2.9% [53, 54]. The difference is significant, but acceptable There is good agreement between the lattice parameters from this thesis and theoretical lattice parameters from studies performed using the CASTEP code [39, 51]. Best agreement between data from ab initio calculations and experimental data was found to be in the work by C. Colinet et al. [37] who performed calculations by the VASP code with a different titanium pseudopotential than was used this work. Calculated internal parameters are consistent with experimental data [28, 29, 33, 56].

From data obtained by calculating enthalpies of formation it was concluded that the C49 phase is the stable structure of $TiSi_2$ at 0 K temperature, the C54 phase is the second most stable structure and the C40 phase is the least stable. Most other studies support this order [37,38,51,55,57]. Calculated enthalpies of formation, with respect to the elements in the standard state were found to be -191.6 kJ/mole of f.u. for C54 phase, -194.7 kJ/mole of f.u. for C49 phase and -186.7 kJ/mole of f.u. for the C40 phase. Compared to data from other studies [38, 51, 55, 57, 58], this is overestimation by about 20-40 kJ/mole of f.u. However when C49 phases is taken as the reference state, enthalpies of formation do conform better within other theoretical data [37, 38, 51, 55, 57].

Values of the calculated bulk moduli were 166.2, 161.0 and 164.9 GPa for the C54, C49 and C40 phases respectively. Bulk moduli of the C54 phase and the C49 phase were overestimated compared to the experimental data [65–67]. A linear muffin-tin orbital study by M. Ekman and O. Vidvuds [64] arrived to similar results and study performed on CASTEP code by T. Wang et al. [63] yielded bulk moduli smaller by 35-55 %. However the experimental data [65–67] vary a lot. Unfortunately no reference data for the bulk modulus of the C40 phase were found.

Obtained density of states fit within data reported by other studies [51, 61, 62]. Only contradiction was the band gap at 2 eV in the density of states belonging to the C49 phase.

Overall the goals of this thesis were fulfilled and will serve as basis for further research on the topic.

Bibliography

[1] C. T. Chuang et al. A schottky-barrier diode with self-aligned floating guard ring. *IEEE T. Electron. Dev.*, 31(10):1482–1486, 1984.

[2] S. Tohyama et al. A high fill factor and progressive scan ptsi schottky-barrier ir-ccd image sensor using new wiring technology. *IEEE T. Electron. Dev.*, 42(8):1433–1440, Aug 1995.

[3] J.P. Gambino and E.G. Colgan. Silicides and ohmic contacts. *Mat. Chem. Phys.*, 52(2):99 – 146, 1998.

[4] R. Beyers and R. Sinclair. Metastable phase formation in titanium-silicon thin films. *J. Appl. Phys.*, 57(12):5240–5245, 1985. cited By 298.

[5] S. Y. Chen et al. Enhancement effect of C40 $TiSi_2$ on the C54 phase formation. *J. Electrochem. Soc.*, 148(12):G734–G737, 2001.

[6] R. G. Parr et al. Molecular orbital calculations of the lower excited electronic levels of benzene, configuration interaction included. *J. Chem. Phys.*, 18(12):1561–1563, 1950.

[7] J. C. Cuevas. Introduction to density functional theory.

[8] M. Born and R. Oppenheimer. Zur quantentheorie der molekeln. *Ann. Phys. Berlin*, 389(20):457–484, 1927.

[9] D. R. Hartree. The wave mechanics of an atom with a non-coulomb central field. part i. theory and methods. *Math. Proc. Cambridge*, 24(1):89–110, 1928.

[10] A. S. Davydov. In *Quantum Mechanics*. Pergamon, second edition edition, 1965.

[11] F. Giustino. *Materials Modelling Using Density Functional Theory: Properties and Predictions*. Oxford University Press, 2014.

[12] D. Branski. Density functional theory calculations for the monolayer–bilayer graphene heterojunctions. Master's thesis, Lehrstuhl für theoretische Festkörperphysik Friedrich-Alexander-Universität Erlangen-Nürnberg, 2014.

[13] W. Koch and M. C. Holthausen. *A chemist's guide to density functional theory*. John Wiley & Sons, 2015.

[14] P. Hohenberg and W. Kohn. Inhomogeneous electron gas. *Phys. Rev.*, 136:B864–B871, Nov 1964.

[15] W. Kohn and L. J. Sham. Self-consistent equations including exchange and correlation effects. *Phys. Rev.*, 140:A1133–A1138, Nov 1965.

[16] M. Born. Zur quantenmechanik der stoßvorgänge. *Zeitschrift für Physik*, 37(12):863–867, 1926.

[17] D. M. Ceperley and B. J. Alder. Ground state of the electron gas by a stochastic method. *Phys. Rev. Lett.*, 45:566–569, Aug 1980.

[18] J. P. Perdew and A. Zunger. Self-interaction correction to density-functional approximations for many-electron systems. *Phys. Rev. B*, 23:5048–5079, May 1981.

[19] M. C. Payne et al. Iterative minimization techniques for ab initio total-energy calculations: molecular dynamics and conjugate gradients. *Rev. Mod. Phys.*, 64:1045–1097, Oct 1992.

[20] B. Meyer et al. The pseudopotential plane wave approach, 2006.

[21] G. Kresse and J. Furthmüller. Efficient iterative schemes for ab initio total-energy calculations using a plane-wave basis set. *Phys. Rev. B*, 54:11169–11186, Oct 1996.

[22] G. Kresse and J. Furthmüller. Efficiency of ab-initio total energy calculations for metals and semiconductors using a plane-wave basis set. *Com.l Mate. Sci.*, 6(1):15 – 50, 1996.

[23] N.N. Greenwood and A. Earnshaw. *Chemistry of the elements*. Pergamon Press, 1984.

[24] D. R. et al. Askeland. *The Science and Engineering of Materials, SI Edition*. CL-Engineering, 6th edition, 2011.

[25] J. Toužín. Stručný přehled chemie prvků, 2003. r01.

[26] R. W. Cahn. Binary alloy phase diagrams–second edition. *Adv. Mater.*, 3(12):628–629, 1991.

[27] J. C. Barbour et al. The thin-film reaction between Ti and thermally grown SiO_2. *J. Appl. Phys.*, 62(6):2582–2584, 1987.

[28] W. Jeitschko. Refinement of the crystal structure of $TiSi_2$ and some comments on bonding in $TiSi_2$ and related compounds. *Acta Crystallogr. B*, 33(7):2347–2348, Jul 1977.

[29] J. F. Jongste et al. Elastic constants and thermal expansion coefficient of metastable C49 $TiSi_2$. *J. Appl. Phys.*, 73(6):2816–2820, 1993.

[30] F et al. La Via. Formation of the TiSi 2 C40 as an intermediate phase during the reaction of the Si/Ta/Ti system. *Appl. Phys. Lett.*, 78(13):1864–1866, 2001.

[31] F. Mammoliti et al. Electrical resistivity and hall coefficient of C49, C40, and C54 $TiSi_2$ thin-film phases. *J. Appl. Phys.*, 92(6):3147–3151, 2002.

[32] T. Káňa et al. Ab initio study of phase transformations in transition-metal disilicides. *Intermetallics*, 19(7):919 – 926, 2011.

[33] K. Tanaka et al. Refinement of crystallographic parameters in transition metal disilicides with the $C11_b$, C40 and C54 structures. *Intermetallics*, 9(7):603 – 607, 2001.

[34] M.G. Grimaldi et al. Kinetics of the C49–C54 phase transition in $TiSi_2$: New indications from sheet resistance, infrared spectroscopy and molecular dynamics simulations. *Microelectro. Eng.*, 37:441 – 448, 1997.

[35] Z. Ma and L. H. Allen. Kinetic mechanisms of the C49-to-C54 polymorphic transformation in titanium disilicide thin films: A microstructure-scaled nucleation-mode transition. *Phys. Rev. B*, 49:13501–13511, May 1994.

[36] R. HwaSung et al. Formation of $TiSi_2$ thin films from chemical vapor deposition using tiI_4. *MRS Proceedings*, 514, 1998.

[37] C. Colinet et al. Ab initio study of the structural stability of $TiSi_2$ compounds. *Appl. Phys. Lett.*, 87(4):041910, 2005.

[38] D.O. Poletaev et al. Ab initio-based prediction and TEM study of silicide precipitation in titanium. *Comp. Mater. Sci.*, 95:456 – 463, 2014.

[39] T. Wang et al. Ab initio comparative study of C54 and C49 $TiSi_2$ surfaces. *Appl. Surf. Sci.*, 252(14):4943 – 4950, 2006.

[40] F. La Via et al. C49 defect influence on the C49–C54 transition. *Microelectron. Eng.*, 70(2–4):215 – 219, 2003. Materials for Advanced Metallization 2003.

[41] F. La Via et al. Defect-induced tetragonalization of the orthorhombic $TiSi_2$ C49 phase: X-ray diffraction and first principles calculations. *Appl. Phys. Lett.*, 78(6):739–741, 2001.

[42] A. et al. Mouroux. Microscopic evidence of C40 and C54 in (Ti,Ta)Si_2: Template mechanism. *Phys. Rev. B*, 60:9165–9168, September 1999.

[43] P. E. Blöchl. Projector augmented-wave method. *Phys. Rev. B*, 50:17953–17979, Dec 1994.

[44] G. Kresse and D. Joubert. From ultrasoft pseudopotentials to the projector augmented-wave method. *Phys. Rev. B*, 59:1758–1775, Jan 1999.

[45] J. Paier et al. The Perdew–Burke–Ernzerhof exchange-correlation functional applied to the g2-1 test set using a plane-wave basis set. *J. Chem. Phys.*, 122(23):234102, 2005.

[46] H. Gruber and E. Krautz. Magnetoresistance and conductivity in the binary system titanium–oxygen. i. titanium oxides with metallic conductivity. *Phys. Status Solidi A*, 69(1):287–295, 1982.

[47] R. M. Wood. The lattice constants of high purity alpha titanium. *Proceedings of the Physical Society*, 80(3):783, 1962.

[48] U. Argaman et al. Thermodynamic properties of titanium from ab initio calculations. *Materials Research Express*, 2(1):016505, 2015.

[49] National Institute of Standards and Technology.

[50] Y. Okada and Y. Tokumaru. Precise determination of lattice parameter and thermal expansion coefficient of silicon between 300 and 1500 k. *J. Appl. Phys.*, 56(2):314–320, 1984.

[51] G. Shao. Prediction of structural stabilities of transition-metal disilicide alloys by the density functional theory. *Acta Materialia*, 53(13):3729 – 3736, 2005.

[52] C.Y. Li et al. The crystallographic stability and anisotropic compressibility of C54-type $TiSi_2$ under high pressure. *J. Phys. Chem. Solids*, 74(9):1291 – 1294, 2013.

[53] T. Yu et al. Structural study of refractory-metal-free C40 $TiSi_2$ and its transformation to C54 $TiSi_2$. *Appl. Phys. Lett.*, 80(13):2266–2268, 2002.

[54] K. Li et al. Identification of refractory-metal-free C40 $TiSi_2$ for low temperature C54 $TiSi_2$ formation. *Appl. Phys. Lett.*, 78(25):3989–3991, 2001.

[55] C. Colinet and J. C. Tedenac. Structural stability of intermetallic phases in the Si–Ti system. point defects and chemical potentials in $D8_8$-Si_3Ti_5 phase. *Intermetallics*, 18(8):1444 – 1454, 2010.

[56] U. Gottlieb et al. Low temperature specific heat measurements of VSi_2, $NbSi_2$ and $TaSi_2$. *Appl. Surf. Sci.*, 73:232 – 236, 1993.

[57] H.J. et al. Seifert. Thermodynamic optimization of the Ti-Si system. *Z. Metallkd.*, 87(1):2–13, 1996.

[58] R.J. Kematick and C.E. Myers. Thermodynamics of the phase formation of the titanium suicides. *Chem. Mater.*, 8(1):287–291, 1996. cited By 25.

[59] N.W. Ashcroft and N.D. Mermin. *Solid State Physics*. HRW international editions. Holt, Rinehart and Winston, 1976.

[60] C. Kittel. *Introduction to Solid State Physics*. Wiley, 2004.

[61] L. F. Mattheiss and J. C. Hensel. Electronic structure of $TiSi_2$. *Phys. Rev. B*, 39:7754–7759, Apr 1989.

[62] P. Ravindran et al. Density functional theory for calculation of elastic properties of orthorhombic crystals: Application to $TiSi_2$. *J. Appl. Phys.*, 84(9):4891–4904, 1998.

[63] T. Wang et al. Ab initio study of the elastic properties of $TiSi_2$. *Materi. Sci. Semicon. Proc.*, 8(4):540 – 544, 2005.

[64] Mathias Ekman and Vidvuds Ozoliņš. Electronic structure and bonding properties of titanium silicides. *Phys. Rev. B*, 57:4419–4424, Feb 1998.

[65] W. Voigt. *Lehrbuch der Kristallphysik: mit Ausschluss der Kristalloptik*. B.G. Teubners Sammlung von Lehrbüchern auf dem Gebiete der mathematischen Wissenschaften mit Einschluss ihrer Anwendungen. J.W. Edwards, 1928.

[66] M. Nakamura. Elastic constants of some transition- metal- disilicide single crystals. *Metall. Mater. Trans. A*, 25(2):331–340, 1994. cited By 39.

[67] C.Y. Li et al. The crystallographic stability and anisotropic compressibility of C54-type $TiSi_2$ under high pressure. *J. Phys. Chem. Solids*, 74(9):1291 – 1294, 2013.